

AIAA 2003-4506
39th Joint Propulsion Conference and Exhibit
Huntsville, AL
July 20-23, 2003

A Review of Analytical Methods for Solid Rocket Motor Grain Analysis

Roy Hartfield, Associate Professor, member AIAA
Rhonald Jenkins, Associate Professor, member AIAA
John Burkhalter, Professor, member AIAA
Winfred Foster, Professor, member AIAA

Aerospace Engineering Department
Auburn University, Auburn, Alabama

Abstract

Analytical methods for solid rocket motor grain design are proving to be tremendously beneficial to some recent efforts to optimize solid-rocket propelled missiles. The analytical approach has fallen out of favor in recent decades; however, for some classes of grains, the analytical methods are much more efficient than grid-based techniques. This paper provides a review of analytical methods for calculating burn area and port area for a variety of cylindrically perforated solid rocket motor grains. The equations for the star, long spoke wagon wheel, and dendrite grains are summarized and the development of the burn-back equations for the short spoke wagon wheel and the truncated star configurations are included. This set of geometries and combinations of these geometries represent a very wide range of possibilities for two-dimensional grain design.

Introduction

In many practical solid rocket motor design efforts, final geometric designs for grains are arrived at using numerical layering techniques. This process is geometrically versatile and imminently practical for cases in which small numbers of final geometries are to be considered. However, for a grain design optimization process in which large numbers of grain configurations are to be considered, generating grids for each candidate design is often prohibitive. For such optimization processes, analytical developments of burn perimeter and port area for two-dimensional grains are critically important.¹⁻³ Most modern texts on solid rocket propulsion do not provide geometric details for grain design.^{4,5} This paper will offer a review of analytical methods for determining burn area and port area as a function of burn distance for a selection of common grain designs.

Analytical developments for solid rocket motor grains were much more prevalent in the decades before widespread use of microcomputers. A summary of one version of the burn back equations for the star grain and for part of one type of wagon wheel can be found in Barrere.⁶ Analytical methods have also been developed for the truncated star and for the dendrite.⁷ Other potential grain configurations are described in NASA publications but very few geometric details are given in such publications.^{8,9}

$$A_{p_1} = 2N \left\{ \begin{aligned} & \frac{1}{2} R_p \sin\left(\frac{\pi\varepsilon}{N}\right) \left[R_p \cos\left(\frac{\pi\varepsilon}{N}\right) + R_p \sin\left(\frac{\pi\varepsilon}{N}\right) \tan\left(\frac{\theta}{2}\right) \right] \\ & - \frac{1}{2} \left(\frac{R_p \sin\left(\frac{\pi\varepsilon}{N}\right)}{\sin\left(\frac{\theta}{2}\right)} - (y+f) \cot\left(\frac{\theta}{2}\right) \right)^2 \tan\left(\frac{\theta}{2}\right) \\ & + \frac{1}{2} (y+f)^2 \left(\frac{\pi}{2} - \frac{\theta}{2} + \frac{\pi\varepsilon}{N} \right) + \frac{1}{2} (R_p + y+f)^2 \left(\frac{\pi}{N} - \frac{\pi\varepsilon}{N} \right) \end{aligned} \right\} \quad (4)$$

Phase II burning occurs when the “flat” segment of Phase I burns out which turns out occur when

$$y+f \geq \frac{R_p \sin\left(\frac{\pi\varepsilon}{N}\right)}{\cos\left(\frac{\theta}{2}\right)} \quad (5)$$

After some development, the burn perimeter for phase II can be written as:

$$S = 2N \left\{ \begin{aligned} & (R_p + f + y) \left(\frac{\pi}{N} - \frac{\pi\varepsilon}{N} \right) \\ & + (y+f) \left(\left(\frac{\pi}{2} - \frac{\theta}{2} + \frac{\pi\varepsilon}{N} \right) - \tan^{-1} \left(\frac{\sqrt{(y+f)^2 - H_1^2}}{H_1} \right) - \frac{\theta}{2} \right) \end{aligned} \right\} \quad (6)$$

The port area for Phase II burning can be represented using sections of two arcs and a triangle by:

$$A_{p_2} = 2N \left\{ \begin{aligned} & \frac{1}{2} R_p \sin\left(\frac{\pi\varepsilon}{N}\right) \left[R_p \cos\left(\frac{\pi\varepsilon}{N}\right) + \sqrt{(y+f)^2 - R_p \sin\left(\frac{\pi\varepsilon}{N}\right)^2} \right] \\ & + \frac{1}{2} (y+f)^2 \left(\left(\frac{\pi}{2} - \frac{\theta}{2} + \frac{\pi\varepsilon}{N} \right) - \tan^{-1} \left(\frac{\sqrt{(y+f)^2 - H_1^2}}{H_1} \right) - \frac{\theta}{2} \right) \\ & + \frac{1}{2} (R_p + y+f)^2 \left(\frac{\pi}{N} - \frac{\pi\varepsilon}{N} \right) \end{aligned} \right\} \quad (7)$$

The area denoted as sliver in Figure 2 may be considered as Phase III burning should there be interest in modeling that burning mode. The equations for that mode of burning are not developed in the literature and some attention is paid to that development here. Figure 3 is a schematic diagram showing one method for analyzing this segment of the burn.

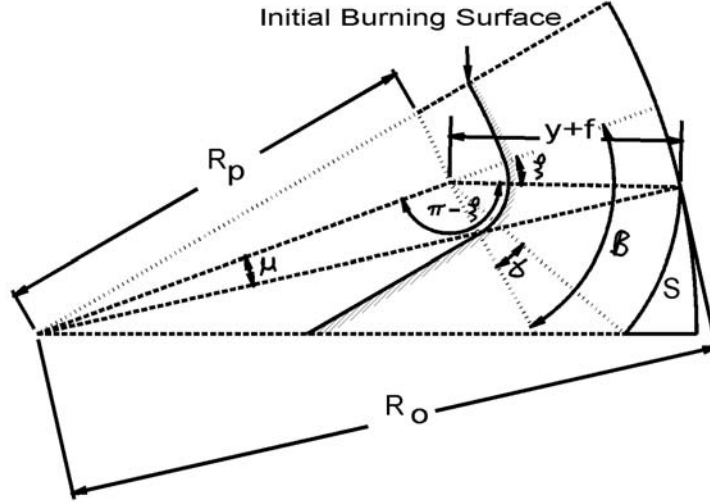


Figure 3. Phase III burning for the star grain

The angles β and γ are used in the development of phase II burning and can be represented as:

$$\beta = \left(\frac{\pi}{2} - \frac{\theta}{2} + \frac{\pi\varepsilon}{N} \right) \quad (8)$$

$$\gamma = \tan^{-1} \left(\frac{\sqrt{(y+f)^2 - R_p \sin\left(\frac{\pi\varepsilon}{N}\right)^2}}{R_p \sin\left(\frac{\pi\varepsilon}{N}\right)} \right) - \frac{\theta}{2} \quad (9)$$

Using the law of cosines, ξ can be determined as follows:

$$\xi = \pi - \cos^{-1} \left[-\frac{R_o^2 - R_p^2 - (y+f)^2}{2R_p(y+f)} \right] \quad (10)$$

The burn perimeter, a section of an arc, becomes:

$$S = 2N[(y+f)(\beta - \gamma - \xi)] \quad (11)$$

The maximum burn distance that can occur can be arrived at using the diagram in Figures 1 and 3 and may be expressed as:

$$y_{\max} = \sqrt{\left(R_o - R_p \cos\left(\frac{\pi\varepsilon}{N}\right) \right)^2 + \left(R_p \sin\left(\frac{\pi\varepsilon}{N}\right) \right)^2} - f \quad (12)$$

A convenient method for determining port area for this phase is to add an arc of angle μ , the arc section corresponding to the burning segment and a triangle through angle $\pi\varepsilon/N$ and then subtract a triangle through angle μ . The angle μ must be determined first and may be written, using the law of sine's, as:

$$\mu = \sin^{-1} \left(\frac{y+f}{R_o} \sin(\pi - \xi) \right) \quad (13)$$

Collecting the areas then results in an expression for the port area.

$$A_p = N \left\{ \begin{aligned} &R_o^2 \left(\frac{\pi}{N} (1 - \varepsilon) + \mu \right) + (y + f)^2 (\beta - \gamma - \xi) \\ &+ R_p \sin \left(\frac{\pi \varepsilon}{N} \right) \left(R_p \cos \left(\frac{\pi \varepsilon}{N} \right) + \sqrt{(y + f)^2 - R_p \sin \left(\frac{\pi \varepsilon}{N} \right)^2} \right) \\ &- R_p \sin(\mu) \left(R_p \cos(\mu) + \sqrt{(y + f)^2 - R_p \sin(\mu)^2} \right) \end{aligned} \right\} \quad (14)$$

“Long Spoke” Wagon Wheels

One of the geometries, not fully explored in the literature, is the wagon wheel. Wagon wheel grain designs can include “spokes” of only one type or “spokes” of two or more types. Wagon wheels with two different sizes of spokes are commonly referred to as dendrites. If the “spokes” burn out from the sides, the designs are referred to herein as “long spoke wagon wheels.” “Short spoke” designs as referred to as Wagon Wheels in which the spokes burn out from the ends. The “long spoke” wagon wheel designs have been developed and included in one form in Barrere. Those results are summarized as follows. To provide a lucid presentation of the wagon wheel geometry, a diagram showing the basic wagon wheel layout is included as Figure 4. The star grain geometry needs only six parameters for a complete definition of the grain cross-section. The wagon wheel grain requires seven parameters. For completeness, a burn back diagram for a sample “long spoke” wagon wheel design is shown in Figure 5.

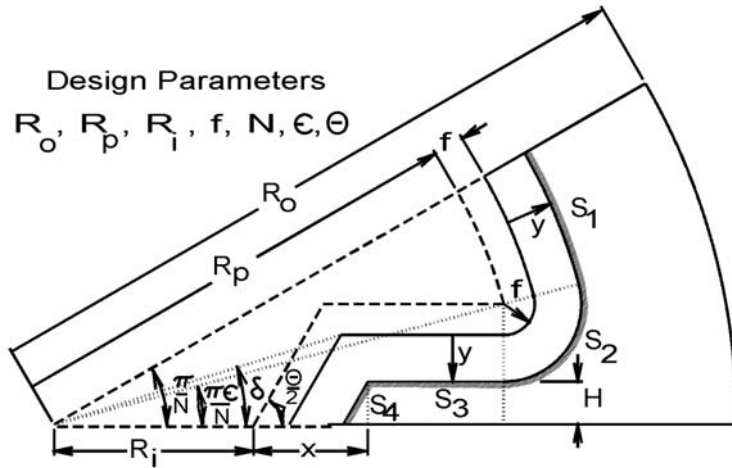


Figure 4. “Long Spoke” wagon wheel geometry

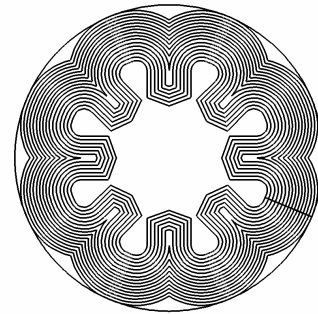


Figure 5: Wagon Wheel

The wagon wheel geometry is more restrictive than the star geometry because the “spokes” must not be allowed to overlap. If the angle δ is defined as the angle between the central axis of the spoke and the edge of the shoulder of the spoke, the relationship defining $\tan(\delta)$ can be written as follows:

$$\tan \delta = \frac{R_p \sin\left(\frac{\pi\epsilon}{N}\right) - f}{R_i + \frac{f}{\sin\frac{\theta}{2}} + \frac{H_{y=0}}{\tan\frac{\theta}{2}}} \quad (15)$$

where H is defined by:

$$H = R_p \sin\frac{\pi\epsilon}{N} - y - f \quad (16)$$

With these definitions, it becomes clear that δ must be less than π/N for the “spokes” to not overlap.

The burn perimeter can be constructed from two arcs and two line-segments and expressed as follows:

$$S = 2N \left\{ \begin{aligned} & \left(R_p + f + y \right) \left(\frac{\pi}{N} - \frac{\pi\epsilon}{N} \right) + (y + f) \left(\frac{\pi}{2} + \frac{\pi\epsilon}{N} \right) \\ & + R_p \cos\frac{\pi\epsilon}{N} - R_i - \frac{y + f}{\sin\frac{\theta}{2}} + \frac{H}{\tan\frac{\theta}{2}} + \frac{H}{\sin\frac{\theta}{2}} \end{aligned} \right\} \quad (17)$$

The port area for phase I burning can be constructed from two arcs and a right triangle with the trapezoidal “spoke” area subtracted off.

$$A_p = 2N \left\{ \begin{aligned} & \frac{1}{2} (R_p + f + y)^2 \left(\frac{\pi}{N} - \frac{\pi\epsilon}{N} \right) + \frac{1}{2} (f + y)^2 \left(\frac{\pi}{2} + \frac{\pi\epsilon}{N} \right) \\ & + \frac{1}{2} R_p^2 \sin\left(\frac{\pi\epsilon}{N}\right) \cos\left(\frac{\pi\epsilon}{N}\right) \\ & - \left(H \left(R_p \cos\frac{\pi\epsilon}{N} - R_i - \frac{y + f}{\sin\frac{\theta}{2}} + \frac{H}{\tan\frac{\theta}{2}} \right) + \frac{1}{2} \frac{H^2}{\tan\frac{\theta}{2}} \right) \end{aligned} \right\} \quad (18)$$

Phase II burning occurs when the “spoke” burns out which is to say when $H = 0$ in which case:

$$y \geq R_p \sin\frac{\pi\epsilon}{N} - f \quad (19)$$

For Phase II, the expression for the arc S_1 is unchanged and both segments S_3 and S_4 are zero. S_2 is an arc of radius $y + f$ and an increasingly smaller angle ϕ which can be defined as:

$$\phi = \frac{\pi}{2} + \frac{\pi\varepsilon}{N} - \cos^{-1} \left(\frac{R_p \sin\left(\frac{\pi\varepsilon}{N}\right)}{y+f} \right) \quad (20)$$

$$S = 2N \left((R_p + f + y) \left(\frac{\pi}{N} - \frac{\pi\varepsilon}{N} \right) + (y+f)\phi \right) \quad (21)$$

The port area for phase II can be written as the sum of the two arc sections and a triangle.

$$A_p = N \left\{ \begin{aligned} & \left((R_p + f + y)^2 \left(\frac{\pi}{N} - \frac{\pi\varepsilon}{N} \right) + (f + y)^2 \left(\frac{\pi}{2} + \frac{\pi\varepsilon}{N} - \cos^{-1} \left(\frac{R_p \sin\left(\frac{\pi\varepsilon}{N}\right)}{y+f} \right) \right) \right) \\ & + R_p \sin\left(\frac{\pi\varepsilon}{N}\right) \left(R_p \cos\left(\frac{\pi\varepsilon}{N}\right) + (y+f) \sin \left(\cos^{-1} \left(\frac{R_p \sin\left(\frac{\pi\varepsilon}{N}\right)}{y+f} \right) \right) \right) \end{aligned} \right\} \quad (22)$$

Phase II ends when the burning first reaches the case. That is when:

$$R_p + f + y > R_o \quad (23)$$

Phase III for the wagon wheel can be modeled exactly as phase III for the star.

“Short Spoke” Wagon Wheel

The short spoke wagon wheel geometry has not been developed in the literature and will be explored in more detail as follows. The geometric determination regarding whether the spoke burns out from the sides or from the end can be made with the aid of the diagram in Figure 6.

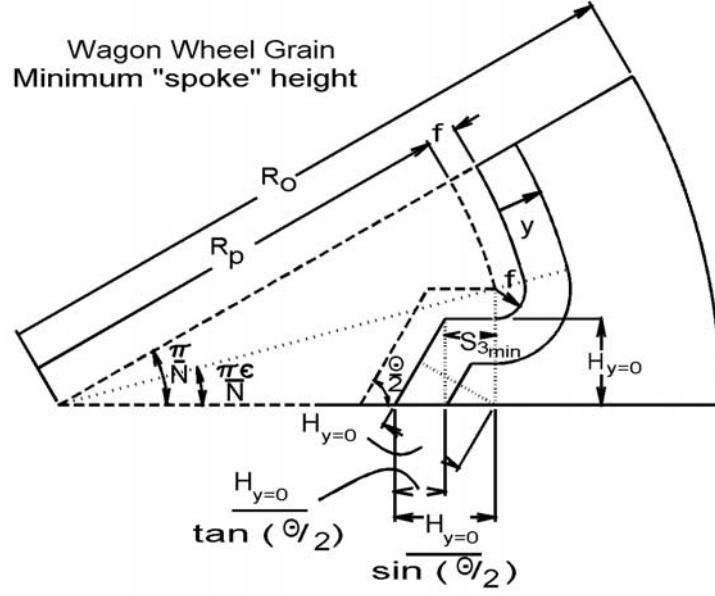


Figure 6. "Short Spoke" Wagon Wheel

For the spoke to burn out from the sides, it must have a minimum height. This effectively limits the value of the burn perimeter segment S_3 as shown in Figure 6. At the transition from long spoke to short spoke, an expression involving the length for S_3 can be written as:

$$R_p \cos\left(\frac{\pi\epsilon}{N}\right) = R_i + \frac{f + H_{y=0}}{\sin\left(\frac{\theta}{2}\right)} = R_i + \frac{R_p \sin\left(\frac{\pi\epsilon}{N}\right)}{\sin\left(\frac{\theta}{2}\right)} \quad (24)$$

Hence, for the "long spoke" development to be appropriate, we must have:

$$R_p \cos\left(\frac{\pi\epsilon}{N}\right) - R_i - \frac{R_p \sin\left(\frac{\pi\epsilon}{N}\right)}{\sin\left(\frac{\theta}{2}\right)} \geq 0 \quad (25)$$

Otherwise, the wagon wheel is of the "short spoke" type.

If S_3 is below the minimum allowable length for the long spoke analysis, the parameters for phase I can be calculated exactly as for the long spoke except that phase I will end when S_3 goes to zero rather than as predicted above. At that point, a phase II burn will occur as depicted in Figure 7. In this phase, S_1 is an arc as predicted above, S_2 is an arc of radius $y + f$ and angle ϕ , S_3 is zero, and S_4 is the remaining slanted face. For this type grain, phase II will begin for a burn distance given by:

$$web1 = \left[R_p \cos\left(\frac{\pi\epsilon}{N}\right) - R_i - \frac{f}{\sin\left(\frac{\theta}{2}\right)} - \frac{R_p \sin\left(\frac{\pi\epsilon}{N}\right) - f}{\tan\left(\frac{\theta}{2}\right)} \right] \tan\left(\frac{\pi - \theta/2}{2}\right) \quad (26)$$

$$s_4 = \frac{R_p \sin\left(\frac{\pi\epsilon}{N}\right) - (y+f)\cos(\beta)}{\sin\left(\frac{\theta}{2}\right)} \quad (34)$$

Finally, the burn perimeter for phase II of a short "spoke" wagon wheel can be written as:

$$S = 2N(S_1 + S_2 + S_4) \quad (35)$$

The port areas for phase II can be assembled as shown in Figure 8.

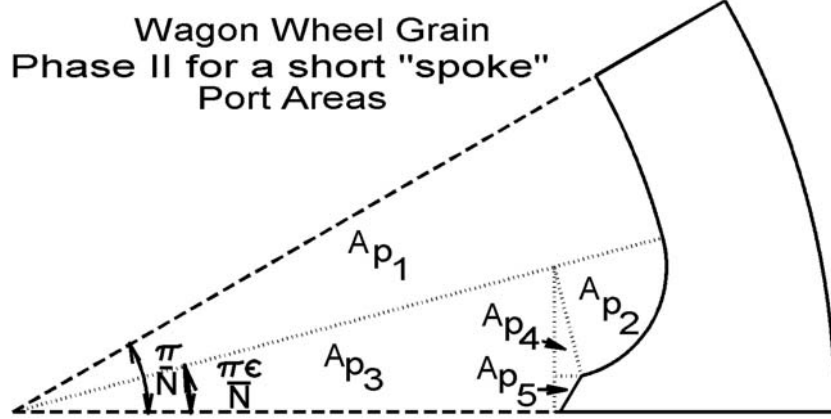


Figure 8. Port Areas for phase II of a short spoke wagon wheel

The areas A_{p_1} , A_{p_2} and A_{p_3} are arcs and triangles which can be written as:

$$A_{p_1} = \frac{1}{2}(R_p + f + y)^2 \left(\frac{\pi}{N} - \frac{\pi\epsilon}{N} \right) \quad (36)$$

$$A_{p_2} = \frac{1}{2}(y+f)^2 \phi \quad (37)$$

$$A_{p_3} = \frac{1}{2}R_p^2 \sin\left(\frac{\pi\epsilon}{N}\right) \cos\left(\frac{\pi\epsilon}{N}\right) \quad (38)$$

The area A_{p_4} is a triangle of area:

$$A_{p_4} = \frac{1}{2}(y+f)^2 \cos\beta \sin\beta \quad (39)$$

For the most general case, A_{p_5} should be constructed as a rectangle with a triangle taken out as follows:

$$A_{p_5} = \left(R_p \sin\left(\frac{\pi\epsilon}{N}\right) - (y+f)\cos\beta \right) \left((y+f)\sin\beta \right) - \frac{1}{2}S_4^2 \sin\left(\frac{\theta}{2}\right) \cos\left(\frac{\theta}{2}\right) \quad (40)$$

The total port area for a short "spoke" phase II burn can then be represented as:

$$A_p = 2N \left(A_{p_1} + A_{p_2} + A_{p_3} + A_{p_4} + A_{p_5} \right) \quad (41)$$

For this type of wagon wheel, phase II will end when S_4 goes to zero provided that the outer radius is large enough. In that case, the condition for ending phase II and going to phase III would be:

$$y = \frac{R_p \sin\left(\frac{\pi\epsilon}{N}\right)}{\cos\beta} - f \quad (42)$$

An explicit closed form for the web thickness for phase II can be developed as follows: At the end of phase II, we can write:

$$(y + f)^2 = \left(R_p \sin\left(\frac{\pi\epsilon}{N}\right)\right)^2 + \left(R_i + \frac{y + f}{\sin\left(\frac{\theta}{2}\right)} - R_p \cos\left(\frac{\pi\epsilon}{N}\right)\right)^2 \quad (43)$$

This equation can be rearranged and written as a quadratic in $y + f$:

$$a(y + f)^2 + b(y + f) + c = 0 \quad (44)$$

where:

$$a = \left(\frac{1}{\sin\left(\frac{\theta}{2}\right)}\right)^2 - 1 \quad (45)$$

$$b = \frac{2\left(R_i - R_p \cos\left(\frac{\pi\epsilon}{N}\right)\right)}{\sin\left(\frac{\theta}{2}\right)} \quad (46)$$

$$c = \left(R_p \sin\left(\frac{\pi\epsilon}{N}\right)\right)^2 + \left(R_i - R_p \cos\left(\frac{\pi\epsilon}{N}\right)\right)^2 \quad (47)$$

The root using the negative term in the quadratic equation provides the physically appropriate solution for the $y_{\text{end phase II}} + f$. The web thickness for phase II can then be written as:

$$\text{web2} = (y_{\text{end phase II}} + f) - f - \text{web1} \quad (48)$$

Phase III for this configuration can be analyzed exactly as phase II for the long spoke configuration. It should be noted that if h is negative, the geometry is over constrained. Such a geometry could be represented by a star grain geometry if the $\theta/2$ parameter were dropped and only six parameters are specified. Both stars and wagon wheels can be represented with the same seven parameters if it is understood that the grain will be a star if h is calculated to be negative and a new value of θ can be calculated for the resulting star geometry.

Dog Bone

The dog bone geometry can generally be represented as a special case of the wagon wheel. Conceptually, this geometry can be used when high initial burn area/chamber pressures are desired. A three-pronged dog bone geometry constructed from a three-spoke wagon wheel grain is shown in Figure 8. Some dog bone geometries have a small circular truncation of the wagon points but for the purposes of preliminary design calculations, the three-spoke wagon treatment is an excellent approximation to the dog bone geometry.

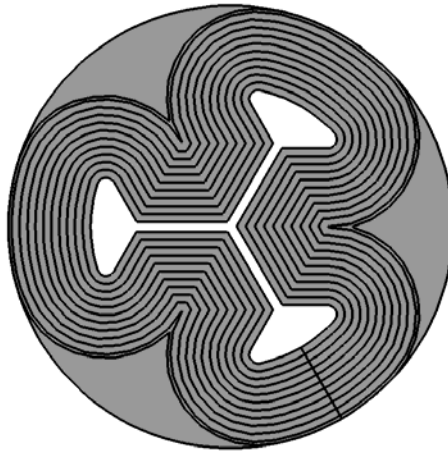


Figure 9. Dog Bone Geometry as Represented by a Three-Spoke Wagon Wheel

Dendrite

The grain cross section ordinarily referred to as a dendrite is a combination of two wagon wheel grains, one of a long spoke design and one of a relatively shorter spoke design. A schematic of a dendrite is shown in Figure 10. By observation, it can be seen that the shorter spokes could be arranged into a 180° arc. Similarly, the longer spokes could be arranged into a 180° arc. Since each of the respective geometries only takes up half of the complete circle, the correct calculations for burn perimeter and port area are obtained by using the total number of points for each of the geometries and then dividing each calculated burn perimeters and port areas by 2 and then summing them for the two geometries. The only additional constraint is that the value of $R_p + f$ must be the same for the two types of spokes.

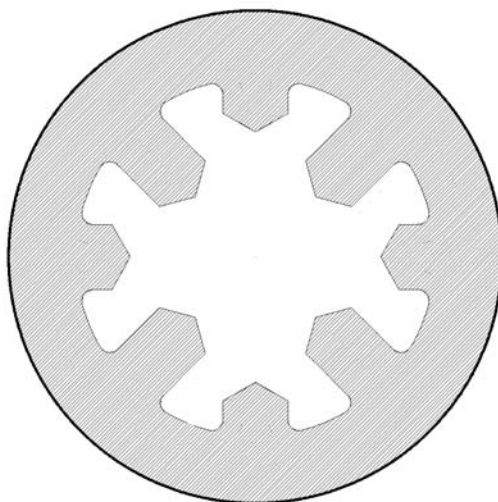


Figure 10. One Representation of a Dendrite

Truncated Star

The truncated star or slotted grain geometry can be defined in using essentially the same variables as a standard star grain. Essentially, the truncated star is a special case of the star grain with the points “bored out” as shown in Figure 11. There are at least four types of truncated stars. The type represented by the diagram in Figure 12 has three burning phases. The first phase ends when the case is reached by the outermost arc. The second phase ends when this outermost arc burns completely out. A second type of truncated star would end with the central arc burning into a point. The geometry that would remain would be describable using the standard star geometry. This would occur for a relatively large number of shallow slots and or for a small value of R_i . A third case could result from phase II ending with the central arc burning out to a point. Finally, a fourth type of truncated star could result from phase II ending due to the shortening of the line segment to a length of zero, with the final phase being the burning of two arced sections. A variety of possible phase III endings could also be considered but in most cases, the chamber pressure will be reduced to near the deflagration limit for most of the phase III burn. The development included in this work will be for the first type. The second type could then very easily be constructed from the first phase of this development coupled with the standard star equations. The remaining types can easily be developed following the methodology used to develop the first type.

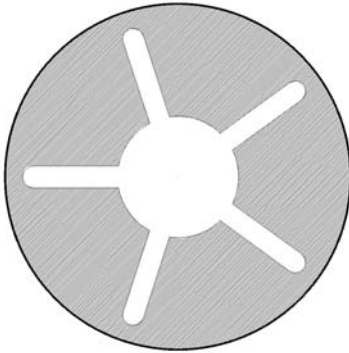


Figure 10. Truncated Star

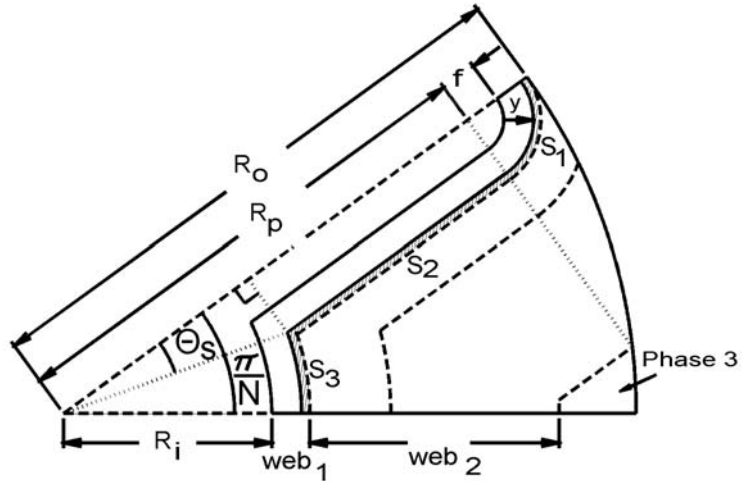


Figure 11. Truncated Star Geometry

It is useful to note that only five parameters are needed to describe this geometry. Since the line segment in the initial phase is by definition a radial line, the parameter ε is not necessary.

For phase I burning of the truncated star, it is useful to define the angle θ_s . From Figure 12, it can be seen that:

$$\theta_s = \sin^{-1} \left(\frac{f + y}{R_i + y} \right) \quad (49)$$

The burning perimeter segments can then be represented by:

$$S_1 = (y + f) \left(\frac{\pi}{2} \right) \quad (50)$$

$$S_2 = R_p - \sqrt{(R_i + f)^2 - (f + y)^2} \quad (51)$$

$$S_3 = (R_i + y) \left(\frac{\pi}{N} - \theta_s \right) \quad (52)$$

The total burn perimeter can then be written as:

$$S = 2N(S_1 + S_2 + S_3) \quad (53)$$

The port area for phase I can be represented as the sum of the arc for S_1 , the arc for S_3 , the triangle defined by θ_s , and a rectangle of sides S_2 and $y+f$.

$$A_p = 2N \left\{ \begin{array}{l} \frac{1}{2}(y+f)^2 \frac{\pi}{2} + \frac{1}{2}(R_i + y)^2 \left(\frac{\pi}{N} - \theta_s \right) \\ + \frac{1}{2}(R_p - S_2)(y+f) + (S_2)(y+f) \end{array} \right\} \quad (54)$$

For phase II, the burn perimeter equations are unchanged with the exception of the fact that the angle for the arc S_1 is reduced from $\pi/2$ to an angle defined as θ_c . By applying the law of cosines to a triangle of sides R_o , R_p and $y+f$, θ_c can be determined as follows:

$$\theta_c = \cos^{-1} \left[-\frac{R_o^2 - R_p^2 - (y+f)^2}{2R_p(y+f)} \right] - \frac{\pi}{2} \quad (55)$$

With θ_c substituted for the angle in the equation for S_1 , the phase I equations can be used for phase II.

The port area for phase II is very similar to the port area for phase I. The only modification to be made is correct for the over prediction of area for the arc S_1 . If the angle θ_p is defined to be the angle between the "vector" R_p and a line segment connecting the geometric center of the grain to the point where the arc S_1 contacts the outer wall, θ_p can be expressed as:

$$\theta_p = \sin^{-1} \left(\frac{y+f}{R_o} \sin \left(\theta_c + \frac{\pi}{2} \right) \right) \quad (56)$$

Using this angle, a correction factor constructed by adding an arc to a triangle and then subtracting a second arc section can be subtracted from the expression for the port area for phase I. The resulting expression for the port area for phase II is:

$$A_p = 2N \left\{ \begin{array}{l} \left[\frac{1}{2}(y+f)^2 \frac{\pi}{2} + \frac{1}{2}(R_i + y)^2 \left(\frac{\pi}{N} - \theta_s \right) \right] - \left[\frac{1}{2}(R_p \sin(\theta_p))R_o \right. \\ \left. + \frac{1}{2}(y+f)^2 \left(\frac{\pi}{2} - \theta_c \right) - \frac{1}{2}R_o^2 \theta_p \right] \\ \left[+ \frac{1}{2}(R_p - S_2)(y+f) + (S_2)(y+f) \right] \end{array} \right\} \quad (57)$$

Summary

The algebraic expressions included in this paper represent the foundation of fast, analytical analysis for cylindrically perforated solid rocket motor grains and combinations of grains. It should be noted that all of these grains including the version of the star which is a cylindrically perforated grain (no star points) can be represented by the same seven parameters to be adjusted by any optimization scheme. If the star parameters are

adjusted properly ($\varepsilon \cong 0$ for example), a cp grain results. If the $\theta/2$ parameter is out of range, a star grain is considered rather than a wagon wheel and the ε parameter could be used such that if its value exceeds unity, a truncated or slotted grain results. Hence, the seven parameters used in this paper can be used as seven adjustable variables describing a tremendous variety of cylindrically perforated grains. If care is taken to maintain a constant web thickness in tapered grains, the equations presented in this paper can be used to accurately model tapered grains provided that linear averages of geometrically similar cross sections are taken between two ends of the grain. The versatility and speed with which grain geometries can be explored using this more classical approach to grain design allows for the available parameter space for motor design to be explored efficiently by any of a variety of design optimization algorithms.

References

1. "Design of a Guided Missile Interceptor Using a Genetic Algorithm", M. Anderson, J. Burkhalter, and R. Jenkins, *AIAA Journal of Spacecraft and Rockets* Vol. 38, No. 1, January 2001, pp. 28-35.
2. "Missile Shape Optimization Using Genetic Algorithms", M. Anderson, J. Burkhalter, and R. Jenkins, *AIAA Journal of Spacecraft and Rockets*, Vol. 37, No. 5, Oct. 2000, pp.663-669.
3. Anderson, M.B., Burkhalter, J.E., and Jenkins, R.M., "Intelligent Systems Approach to Designing an Interceptor to Defeat Highly Maneuverable Targets", AIAA Paper 2001-1123, presented at the 39th Aerospace Sciences Meeting and Exhibit, Reno, NV, January 2001.
4. Davenas, A., Solid Rocket Propulsion Technology, Pergamon Press, Oxford, 1993.
5. Sutton, G., and Biblarz, O., Rocket Propulsion Elements, Seventh Edition, John Wiley & Sons, Inc, New York, 2001.
6. Barrere, M., Jaumotte, A., Veubeke, B., and Vandenkerckhove, J., Rocket Propulsion, Elsevier Publishing Company, Amsterdam, 1960.
7. Sforzini, Richard H., "Notes on Solid-Propellant Rocket Motors Including Jet Propulsion Fundamentals," Auburn University, May 1980.
8. "Solid Propellant Grain Design and Internal Ballistics", NASA SP 8076 (library.msfc.nasa.gov/cgi-bin/lsp8000)
9. "Solid Rocket Motor Performance Analysis and Prediction", NASA SP 8039 (library.msfc.nasa.gov/cgi-bin/lsp8000)